9-1-2006

A New Class of Miniature Embedded Inverted-F Antennas (IFAs) for 2.4 GHz WLAN Application

Mohammed Z. Azad
Motorola, Inc., azad@motorola.com

Mohammod Ali
University of South Carolina - Columbia, alimo@engr.sc.edu

Publication Info

Published in *IEEE Transactions on Antennas and Propagation*, Volume 54, 2006, pages 2585-2592.
http://ieeexplore.ieee.org/xpl/RecentIssue.jsp?punumber=8

A New Class of Miniature Embedded Inverted-F Antennas (IFAs) for 2.4 GHz WLAN Application

Mohammed Ziaul Azad, *Student Member, IEEE*, and Mohammod Ali, *Senior Member, IEEE*

***Abstract*—A new class of miniature printed embedded inverted-F antennas are proposed for operation in the 2.4–2.485 GHz wireless local-area network band. One of the proposed antennas on FR4 substrate (dielectric constant = 4.4) measures 9.2 mm by 4.1 mm and has a bandwidth of 3.5%. The peak gain of this antenna is 1.4 dBi. An overall size reduction of 70% is achieved compared to a conventional inverted-F antenna. Effects of dielectric loss tangent and material conductivity on the bandwidth and efficiency of these antennas are also investigated. Finally, two embedded antenna elements are analyzed to demonstrate the feasibility for a decoupled antenna pair consisting of switched and combining diversity schemes.**

***Index Terms*—Antenna, diversity, Hilbert, wireless.**

I. Introduction

THE rapid proliferation of wireless communications has created a strong demand for small internal antennas for mobile phones operating in 900/1900 MHz band applications [1]–[11]. Many wireless devices, such as laptops, mobile phones, and personal digital assistants (PDAs), also have Bluetooth or IEEE wireless local-area network (WLAN) functionalities integrated within them. Antenna choices for such applications include surface-mount planar inverted-F antennas (PIFAs) [12], packaged inverted-F antennas (IFAs) [13], packaged microstrip patches [14], and the embedded (printed directly on the printed circuit board) IFAs [15], [16]. Other examples of board-mounted IFA for 2.4 and 5 GHz WLAN applications can be found in [17]–[20].

Due to the limited space availability on the printed circuit board (PCB) of a wireless device, antenna miniaturization is crucial. Furthermore, the presence of internal mobile phone and GPS antennas on or near the same circuit board limits the space availability and creates potential problem of undesired coupling between antennas. In [17], a meander-line antenna was proposed to conserve space. Fractal and Hilbert-shaped antennas were proposed to achieve antenna size reduction [21]–[24]. Recently, we introduced a miniaturized (50% smaller than a conventional PIFA) modified Hilbert PIFA for 900/1900 MHz band mobile phone application [10].

In this paper, we investigate the properties of a new class of miniature embedded IFAs: the Hilbert IFAs. We explore these antennas with a concentration on the 2.4 GHz IEEE WLAN frequency band. This paper is organized as follows. First, two miniature Hilbert IFAs are designed for application in the 2.4–2.485 GHz band within 2.5:1 voltage standing-wave ratio (VSWR). An antenna is fabricated on FR4 and tested to validate performance. Second, a simple intuitive analytical design approach is presented based on the equivalent inductance concept. Using this approach, the operating frequencies of Hilbert IFAs on various substrates can be easily predicted within 5% of the frequency predicted using full-wave simulators. Third, the effects of conductor and dielectric loss on the bandwidth and efficiency of embedded antennas are investigated. Fourth, an example of a surface mountable Hilbert PIFA is presented that can be used in lieu of the proposed embedded IFA where removal of the PCB ground plane should be avoided. Finally, the prospects of using the embedded antennas as a decoupled antenna pair and in two types of diversity schemes are investigated, which indicate promising potentials.

Manuscript received May 17, 2005; revised January 27, 2006. This work was supported in part by the National Science Foundation under Career Award ECS-0237783.

The authors are with the Department of Electrical Engineering, University of South Carolina, Columbia, SC 29208 USA (e-mail: alimo@ engr.sc.edu; azad@engr.sc.edu).

Digital Object Identifier 10.1109/TAP.2006.880710

II. Antenna Design

The geometry of the proposed Hilbert IFA is shown in Fig. 1. The antenna trace is printed on top of a dielectric substrate. The ground plane underneath the antenna trace is removed. Everywhere else the ground plane is present. For visualization only, the substrate beneath the antenna is shown as removed in Fig. 1(a). The Hilbert geometry allows a longer electrical length, which helps achieve miniaturization.

Fig. 1(b) and (c) depict two fourth iteration order Hilbert curves with slightly different trace widths. The HFSS model consists of the antenna on an FR4 PCB measuring $L = 110$ mm, $W = 50$ mm, $h = 1.5$ mm. The antenna is fed using a vertical metal strip, which is excited using a 50 Ω lumped gap source. The shorting pin is connected to the ground plane. In practical application the antenna can be fed through a strip line from a different layer with the help of a vertical via. As a starting design using HFSS, the trace length at the end of each antenna was adjusted to achieve operation at around 2.45 GHz.

III. Results

First, a fourth iteration order Hilbert IFA with trace width $= 0.25$ mm was designed for operation at 2.45 GHz. Parameters of this antenna are listed in Table I. The distance between the nearest ground conductor and the antenna was fixed at $d_1 = d_2 = 1$ mm. This antenna (antenna A) required an area of 38 mm^2, 70% smaller than a conventional straight conductor IFA [15]. Computed VSWR and input impedance data for this antenna are shown in Fig. 2. The parameter s (separation between the feed and the shorting pin) was varied by moving the location of the feed point. Increasing s as 0.75, 1.25, 1.75, and 2.25 mm increases the operating frequency as 2.41, 2.43, 2.46, 2.48 GHz,

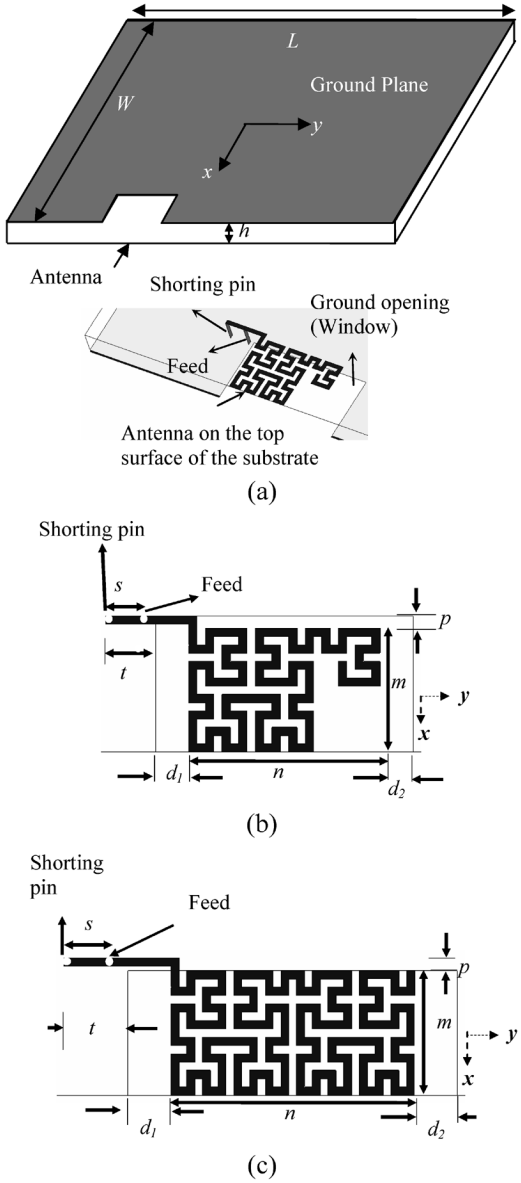

Fig. 1. Proposed miniaturized Hilbert IFAs. (a) Antenna placement and orientation, (b) antenna A, and (c) antenna B.

TABLE I
ANTENNA PARAMETERS (mm)

Antenna	m	n	s	t	p	Area (mm^2)
A	3.75	5.75	1.25	1.5	0.375	38
B	2.7	5.58	1.10	1.5	0.274	27

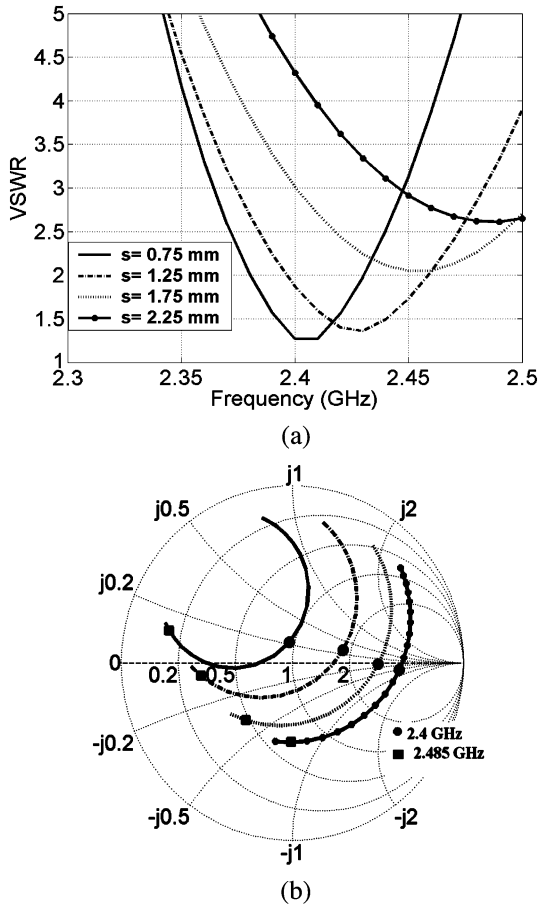

Fig. 2. Computed (a) VSWR and (b) impedance for antenna A with feed to shorting pin spacing, with s as the parameter.

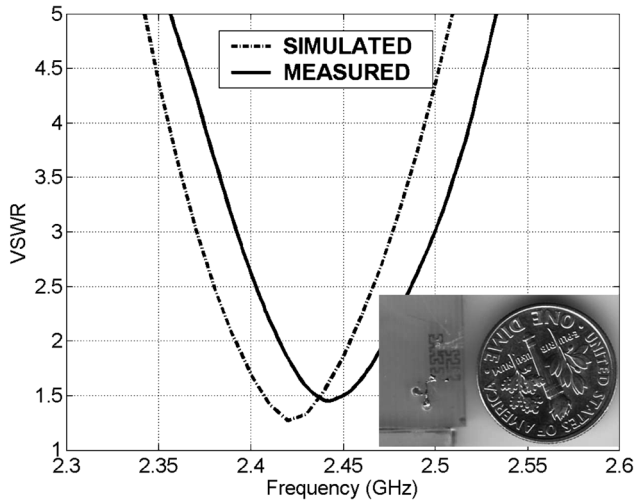

Fig. 3. Computed and measured VSWR for antenna A.

respectively, as the antenna effective length decreases. The increase in frequency can be attributed to the decrease in antenna electrical length.

The important role that the parameter s plays can be understood from the impedance plots of Fig. 2(b). By adjusting this parameter (s), one may control the value of the shunt inductance given by the shorting pin in order to obtain optimum impedance matching. It is evident from Fig. 2(b) that increasing s increases the additional shunt inductance, which in turn moves the resulting antenna input impedance to the lower half of the Smith chart. Thus increasing s results in poor VSWR performance for this case. The simulated antenna (antenna A) was fabricated (1 oz copper) and measured on a 1.5-mm-thick FR4 substrate. These results are shown in Fig. 3. The agreement between the computed and measured data is good. The slight difference in the operating frequency and bandwidth between the simulated and measured prototypes may have resulted from the variation

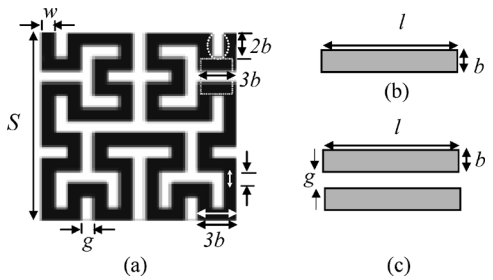

Fig. 4. (a) The Hilbert curve with its design parameters, (b) a flat strip conductor, and (c) parallel flat strip conductors.

in the dielectric constant of the FR4 material and the resolution of our chemical etching process. A photograph of the fabricated antenna shown as an inset in Fig. 3 clearly shows its miniature size (less than the size of one-quarter of a dime). The measured bandwidth of the antenna within 2.5:1 VSWR is 85 MHz (3.5%), which clearly satisfies the Bluetooth or IEEE 802.11 b WLAN application.

To examine the effect of trace width on the operating frequency and bandwidth of the Hilbert IFA, an antenna with trace width of 0.18 mm (antenna B) (which leads to a smaller antenna size compared to antenna A) was designed for operation at 2.45 GHz. The geometry of this antenna is shown in Fig. 1(c). This fourth iteration order Hilbert IFA requires a surface area of 27 mm^2 and has a bandwidth of 3.3%. The bandwidth of antenna B is slightly narrower than antenna A (3.3% compared to 3.5%).

IV. Simple Design Procedure for a Hilbert IFA

For the Hilbert antenna shown in Fig. 4, the strip width w and the spacing between the strips g can be used to determine the external dimension S of the antenna [see Fig. 4(a)], which can be expressed as [25]

$$S = 2^k(w+g) - g \tag{1}$$

where k is the iteration order of the Hilbert curve. For instance, for antenna B $S = 2^4(0.18+0.18) - 0.18 = 5.58$ mm [see Table I].

Referring to Fig. 4, a Hilbert antenna can be decomposed into parallel and nonparallel transmission lines. Consider $w = g = b$. In that case the antenna consists of two types of parallel transmission lines, one with length $2b$ and the other with length $3b$. The antenna also contains other lines that do not fall under the parallel line definition. The design of a Hilbert IFA can proceed based on the inductance equivalence concept introduced in [26]. This requires computing the inductance of the Hilbert antenna using simple formulas. For instance, consider the transmission line embodiments illustrated in Fig. 4(b) and (c).

The self-inductance of a flat wire or strip of width b and length l (conductor is infinitesimally thin) can be calculated as [27]

$$L = 2\times 10^{-3}\times l\left[\ln\left(\frac{l}{b}\right) + 1.193 + 0.2253\times\left(\frac{b}{l}\right)\right] \quad \text{(nH)} \tag{2}$$

where l and b are in centimeters. Similarly, the total inductance of the parallel lines is given by [27]

$$L_{total} = 2L - 2M \quad \text{(nH)} \tag{3}$$

where L is the self-inductance of each parallel strip as defined in (2) and M is the mutual inductance between them such as

$$M = 0.002l\left[\ln\left(\frac{2l}{g}\right) - \log_e k - 1 + \frac{g}{l} - \frac{g^2}{4l^2}\right] \quad \text{(nH)} \tag{4}$$

where $log_e k$ is very small compared to other parameters in (4) and can be found in [28] for different values of b/c. Here b, l, c (conductor thickness) and g are in centimeters. In our case, we used $\log_e k = 0$.

As mentioned, the design of a Hilbert IFA can proceed based on the inductance equivalence concept. First, consider a straight conductor IFA as described in [15]. We have found from a number of HFSS simulations that the resonant length (l_{res}) of a straight conductor IFA that consists of the length of the antenna trace and the feed pin is approximately $0.22\lambda_{\text{g}}$, where $\lambda_g = c/(f\sqrt{\varepsilon_{reff}})$ and $\varepsilon_{reff} \approx (\varepsilon_r + 1)/2$. Here $c = 3\times 10^8$ m/s, f is the operating frequency in hertz, and $\boldsymbol{\varepsilon_r}$ is the dielectric constant of the substrate. A simple design procedure can be summarized as follows.

- Calculate the inductance of the Hilbert IFA using (2)–(4).
- Substitute the total inductance L_{total} calculated above in (5) below to determine the resonant frequency of the antenna. Note that the inductance given by the right-hand side of (5) is equivalent to the inductance of a straight conductor IFA with given length l_{res} and width $(b = w)$.

$$L_{\text{total}} = 2\times 10^{-3}\times l_{res}\left[\ln\left(\frac{l_{res}}{b}\right) + 1.193 + 0.2253\times\left(\frac{b}{l_{res}}\right)\right] \quad \text{(nH)} \tag{5}$$

where l_{res} and b are in centimeters. For instance, the inductance obtained for a specific Hilbert IFA once substituted in (5) will give l_{res} from which the operating frequency of the antenna can be calculated since $l_{res} = 0.22\lambda_g$ and the other parameters are defined above.

To test the validity of the design principles described above, several Hilbert IFAs were analyzed. This study falls into two cases.

Case 1) The substrate dielectric constant (FR4) was fixed while the Hilbert geometry was varied.

Case 2) The Hilbert geometry was fixed while the substrate dielectric constant was varied.

First, for each case, the operating frequency of the antenna was calculated using the principle outlined above and then compared with the frequency computed from HFSS simulation. The results of Case 1) are listed in Table II and those of Case 2) are given in Table III. From Tables II and III, we can clearly see that the maximum error in operating frequency using the proposed technique is less than or equal to 5%.

TABLE II
PREDICTED VERSUS SIMULATED OPERATING FREQUENCIES OF DIFFERENT RESONANT HILBERT IFAS ON FR4 SUBSTRATE; N_1—NUMBER OF PARALLEL LINES WITH LENGTH $l = 2b$, N_2—NUMBER OF PARALLEL LINES WITH LENGTH $l = 3b$, N_3—NUMBER OF NONPARALLEL LINES WITH LENGTH $l = b$, AND $N_4 = 8$ (NUMBER OF NONPARALLEL LINES WITH LENGTH $l = 3b$). SUBSTRATE thickness $= 1.5$ mm

Geometry	$w = g$ (mm)	N_1	N_2	N_3	Inductance, $\times 10^{-11}$(H)	Antenna operating frequency, GHz (HFSS)	Antenna operating frequency, GHz (this method)	% Error
	0.30	31	11	30	2.9761	1.575	1.615	2.4
	0.25	19	6	19	1.8186	2.45	2.47	0.8
	0.18	32	12	30	1.7826	2.45	2.58	5.0
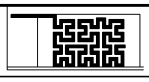	0.10	24	8	23	0.956	5.2	4.96	4.8

TABLE III
PREDICTED VERSUS SIMULATED OPERATING FREQUENCIES OF A HILBERT IFA (ANTENNA A) ON SEVERAL SUBSTRATES; total Hilbert inductance $= 1.8186 \times 10^{-11}$ H. SUBSTRATE thickness $= 1.5$ mm

$w = g$ (mm)	ε_r	N_1	N_2	N_3	HFSS (GHz)	This method (GHz)	% Error
0.25	10.2	19	6	19	1.74	1.72	1.1
0.25	4.5	19	6	19	2.45	2.43	0.8
0.25	2.2	19	6	19	3.05	3.2	4.6

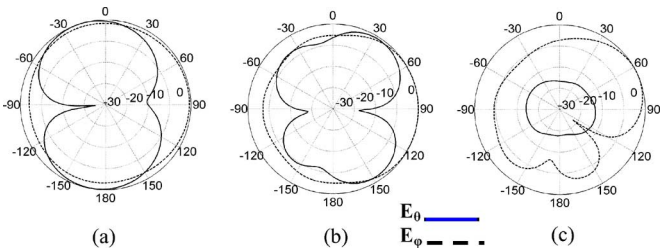

Fig. 5. Computed radiation patterns of antenna A at 2.45 GHz. (a) $\varphi = 0°$ (xz plane), (b) $\varphi = 90°$ (yz plane), and (c) $\theta = 90°$ (xy plane).

V. RADIATION CHARACTERISTICS

Computed normalized radiation patterns for antenna A are shown in Fig. 5. Patterns were computed at 2.45 GHz. It is clear from Fig. 5(a) that the E_φ component is fairly uniform. The E_θ component has a figure-eight pattern. From the yz-plane pattern shown in Fig. 5(b), it is apparent that the E_θ component will reinforce the E_φ component in a multipath propagation environment. The xy-plane patterns are shown in Fig. 5(c) from which it can be seen that the E_φ component varies between -10 to 0 dB throughout the entire angular region except two pockets between $\varphi = -162°$ to $-176°$ and $\varphi = 117°$ to 137°. The current distribution on antenna A is shown in Fig. 6. The current is uniformly distributed over the entire conductor length probably due to the orientation of the Hilbert antenna with respect to the ground plane. Fairly strong currents are concentrated on the nearby ground conductor as well as on the antenna conductors that are near the ground plane. This illustrates the dominant role the ground plane plays in the radiation mechanism of the antenna.

Fig. 6. Current distribution of antenna A at 2.45 GHz.

VI. EFFECTS OF CONDUCTOR AND DIELECTRIC LOSS

The characteristics of antenna A were investigated in more detail in this section. First, antenna efficiency was computed by varying the dielectric loss tangent $\tan\delta$ as 0, 0.012, and 0.02, respectively. The ideal case of $\tan\delta = 0$ was considered as a limit while $\tan\delta = 0.02$ was used to represent the most commonly used FR4 material at 2.4 GHz. An intermediate value of $\tan\delta = 0.012$ was also used to observe the effect of other low-loss dielectrics. From Fig. 7, it is clear that the antenna bandwidth increases as loss tangent is increased. This is expected since the antenna quality factor (Q)[1] decreases when the losses in the system increase. For $\tan\delta = 0$, bandwidth is only 1.3%. It can be observed that the spread in the impedance locus for $\tan\delta = 0$ is much larger than the spread for other values of $\tan\delta$. This clearly indicates that the potential for bandwidth deceases with decreasing $\tan\delta$ even if impedance matching is employed. Thus the bandwidth attained by ultraminiature embedded antennas may be partly due to the lossy nature of the dielectric substrate on which they are printed on.

A study of the efficiency for antenna A was conducted as function of dielectric losses. The antenna trace was modeled using a perfect electric conductor (PEC). Antenna efficiency is 100% when $\tan\delta = 0$. As $\tan\delta$ increases to 0.012 and 0.02, efficiency decreases to 71% and 58%, respectively, at 2.45 GHz. Antenna peak gain decreases from 2.0 to 1.5 to 1.4 dBi as loss tangent increases from 0 to 0.012 to 0.02, respectively, at 2.45 GHz.

[1]Bandwidth varies inversely with Q

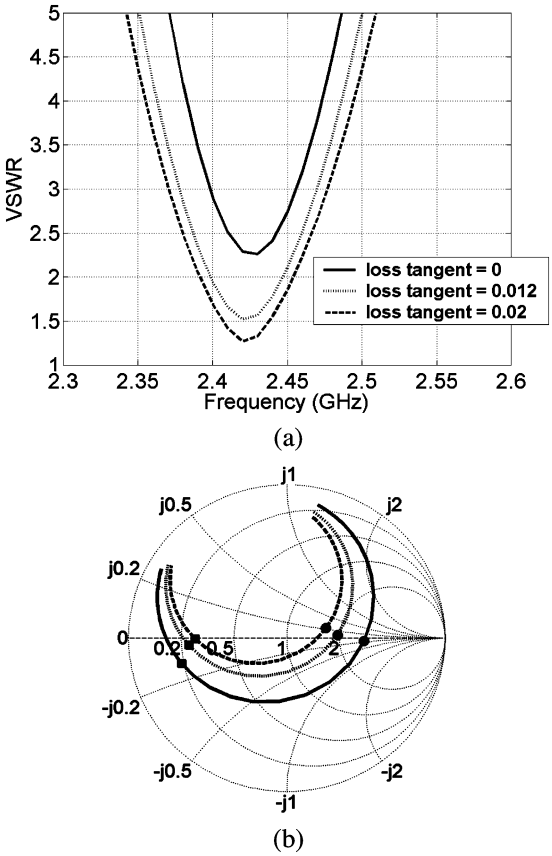

Fig. 7. Computed (a) VSWR and (b) impedance of antenna A with $\tan\delta$ as the parameter.

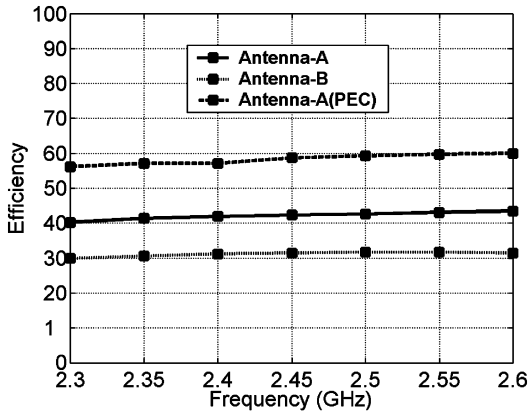

Fig. 8. Computed efficiency for different antennas with copper as the conductor $(\tan\delta = 0.02)$.

The effect of conductor loss is illustrated in Fig. 8 when $\tan\delta = 0.02$ is fixed. Two scenarios are considered: 1) comparing losses between PEC and copper for antenna A and 2) comparing losses between antennas A and B (both copper). For antenna A with $\tan\delta = 0.02$, efficiencies are 58% and 42% for PEC and copper, respectively. Thus there is a 16% reduction in efficiency for copper. Comparing the efficiency degradation due to conductor and dielectric, it is clear that low-loss dielectric should be preferred. Comparing between two antennas (antennas A and B) both on FR4 with $\tan\delta = 0.02$ and with copper as the conductor, the efficiencies are 42%, and 31%, respectively. Clearly the smaller antenna (antenna B) will have lower efficiency. Corresponding peak gain values for antennas A and B are 1 and 0.70 dBi, respectively, for copper.

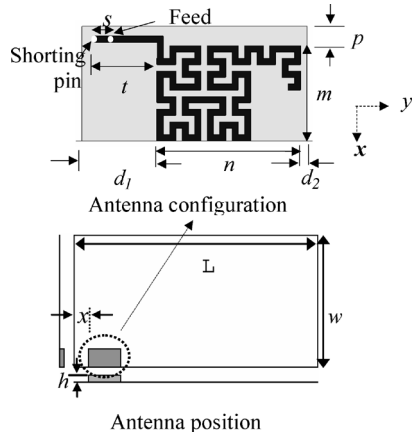

Fig. 9. Geometry and position of surface-mount antenna. Design parameters are substrate thickness $= h$, $m = 3.75$ mm, $n = 5.75$ mm, $s = 0.5$ mm, $x = 7$ mm, $d_1 = 3$ mm, $d_2 = 0.25$ mm, $p = 1.25$ mm, $t = 2.5$ mm.

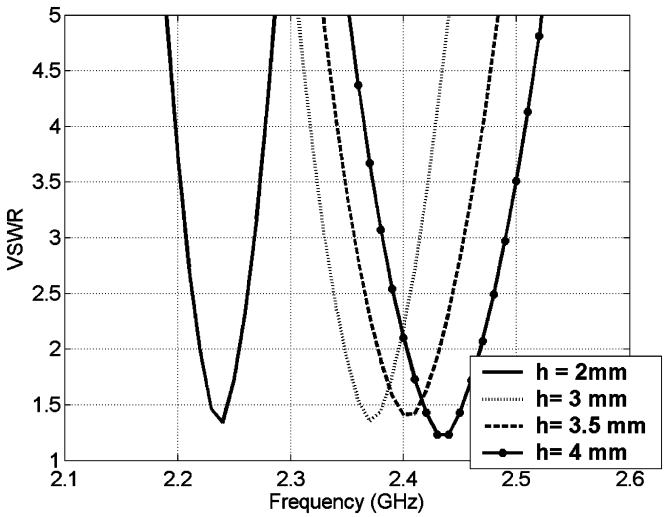

Fig. 10. Computed VSWR data for different heights of a surface mount IFA. Antenna is printed on FR4 substrate $(\varepsilon_r = 4.4)$.

VII. Surface-Mount Antenna

In some circumstances when the embedded antenna introduced in Fig. 1 cannot be used because the metal ground underneath the antenna cannot be removed, a surface-mount antenna can be used. The surface-mount antenna can be manufactured as a separate component and then placed on the PCB as shown in Fig. 9. The Hilbert surface mount PIFA shown in Fig. 9 has $w = g = 0.25$ mm and measures 9 mm by 4.5 mm by 4 mm. This antenna has metal underneath it. Fig. 10 shows VSWR data with the antenna height h as the parameter. It is observed that $h = 4$ mm gives 3.7% bandwidth, 1.4 dBi peak gain, and 45% efficiency (copper trace and $\tan\delta = 0.02$). The operating frequency decreases and the bandwidth becomes narrow as the height decreases to $h = 2$ mm (bandwidth $= 2.2\%$).

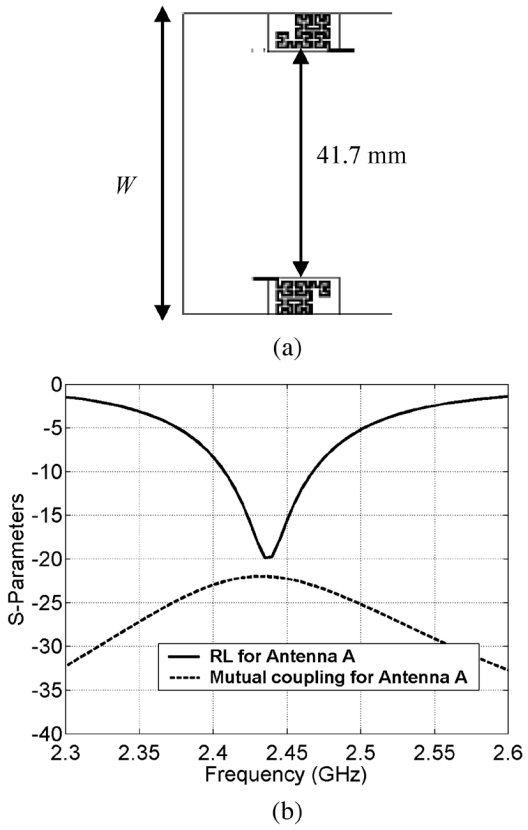

Fig. 11. (a) Proposed decoupled antenna pair and (b) computed S-parameters of decoupled antenna pair.

VIII. Decoupled Antenna Pair

It is well known that having two separate antennas (each functioning independently) over a single antenna is advantageous since it eliminates the need for a diplexer. However, if the inter-antenna spacing is small, which is generally the case for mobile terminals, the mutual coupling between the antenna elements can be strong[2]. To avoid pattern degradation, mutual coupling (S_{21}) of approximately -20 dB or lower is generally recommended [29]–[31]. Since our proposed miniature Hilbert IFAs occupy minimal space, we can achieve greater distance between two antennas, which has the potential for low mutual coupling. This was examined by computing the S-parameters of two IFAs (antenna A) as shown in Fig. 11. The mutual coupling between the Hilbert IFAs is less than -22 dB.

IX. Dual Planar Integrated Inverted F-Antenna Diversity System

In this section, we examine the feasibility of using two Hilbert IFAs for diversity application in the 2.45 GHz band. The quality of a diversity antenna system is measured using the envelope correlation coefficient [1], [32], [33] ρ_{eij} of two signals which can be characterized by the complex correlation coefficient $\rho_{cij}(i,j=1,2)$ [33] with $\rho_{eij} \approx |\rho_{cij}|^2$, where ρ_{cij} can be found from the radiation patterns of the antenna elements and the statistics of the channel (ρ_{cij}^{rp}) or from the mutual coupling between the two antennas (ρ_{cij}^{mc}). The latter quantity ρ_{cij}^{mc} can be estimated using normalized mutual resistance $r_{ij} = Re(Z_{ij})/Re(Z_{ii})$ (where Z_{ij} is the standard two port impedance) and $\rho_{cij}^{mc} = r_{ij}$ [29], [30]. The quantity ρ_{cij}^{rp} can be calculated as [1]

[2]The smaller the number, the weaker the mutual coupling, the strongest being $S_{21} = 0$ dB.

TABLE IV
Envelope Correlation Coefficient and MEG Ratio

Diversity Scheme	Envelope Correlation Coefficient ρ_e		MEG
	Mutual Coupling	Radiation Pattern	
Swithced	N/A	0.015	0.9957
Combining/ MIMO	0.02	0.032	0.9963

$$\rho_{cij}^{rp} = \frac{\int_0^{2\pi} A_{ij}(\varphi)d\varphi}{\left[\int_0^{2\pi} A_{ii}(\varphi)d\varphi \int_0^{2\pi} A_{jj}(\varphi)d\varphi\right]^{1/2}} \tag{6}$$

$$A_{ij}(\varphi) = \Gamma E_{\theta i}\left(\frac{\pi}{2},\varphi\right) E_{\theta i}^{*}\left(\frac{\pi}{2},\varphi\right) + E_{\varphi i}\left(\frac{\pi}{2},\varphi\right) E_{\varphi i}^{*}\left(\frac{\pi}{2},\varphi\right) \tag{7}$$

where E_θ and E_φ are the θ and φ polarized electric field patterns of the antennas on the azimuth plane and Γ is the cross-polarization discrimination of the incident field. The asterisk denotes complex conjugate quantities. In mobile wireless environment, $\Gamma = 1$ [33]. For a good diversity system, it is required that $\rho_{eij} < 0.5$.

We studied the performance of our miniature Hilbert IFA under two types of diversity schemes: 1) combining/multiple-input multiple-output (MIMO) diversity and 2) switched diversity. In the combining/MIMO scheme, one antenna element is directly fed while the other is terminated with a 50 Ω load. In the switched diversity scheme, one antenna is fed while the other is open-circuited. The orientation of the two antennas and the spacing between them are as illustrated in Fig. 11(a). For either of these two cases we found $\rho_{eij} < 0.5$ (see Table IV), which satisfies the condition for good diversity.

Also the mean effective gain (MEG) under both of these schemes was calculated using (8) [29], [30]

$$\text{MEG} = \int_0^{2\pi} \left[\frac{\Gamma}{1+\Gamma} E_\theta(\pi/2,\phi) + \frac{1}{1+\Gamma} E_\phi(\pi/2,\phi)\right] d\phi. \tag{8}$$

For good diversity performance, the ratio of the MEG of the antennas (MEG1/MEG2) should be close to unity. Computed MEG ratios in the two diversity schemes using the Hilbert IFAs are also listed in Table IV.

Finally the radiation patterns under the switched diversity scheme are shown in Fig. 12. Clearly when one antenna shows low gain performance, the other antenna compensates for it. As isolation between the antennas is very good, we achieve very

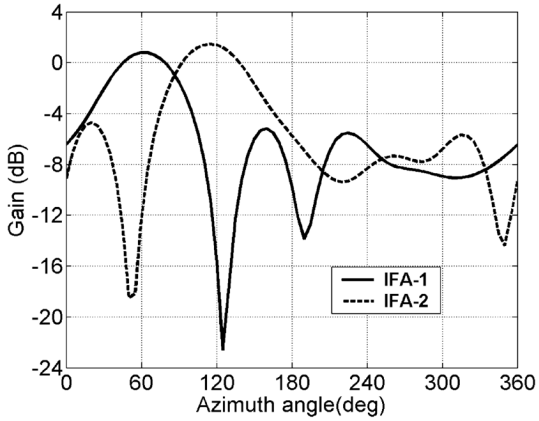

Fig. 12. Computed antenna gain patterns in the azimuth plane (xy plane) under the switched diversity scheme.

similar performance while using the same structure in combining/MIMO diversity scheme.

X. Conclusion

A new class of miniature embedded inverted-F antennas are introduced for operation in the 2.4–2.485 GHz WLAN band. One of the proposed antenna on FR4 substrate (dielectric constant $= 4.4$) is only 9.2 mm by 4.1 mm and has a bandwidth of 3.5% with peak gain of 1.4 dBi. This antenna is at least 70% smaller than a conventional embedded inverted-F antenna. A new concept to determine the operating frequencies of Hilbert IFAs is introduced, which uses the principle of inductance equivalence. A detailed study of the antenna performance as a function of substrate loss tangent and material conductivity is presented. Finally, examples of decoupled antenna diversity schemes are given where the isolation between antennas is better than -20 dB.

References

[1] M. A. Jensen and Y. Rahmat-Samii, "Performance analysis of antennas for hand-held transceivers using FDTD," *IEEE Trans. Antennas Propag.*, vol. 42, pp. 1106–1113, Aug. 1994.

[2] C. R. Rowell and R. D. Murch, "A capacitively coupled PIFA for compact mobile telephone handsets," *IEEE Trans. Antennas Propag.*, vol. 45, pp. 837–842, May 1997.

[3] K. L. Virga and Y. Rahmat-Samii, "Low-profile enhanced-bandwidth PIFA antennas for wireless communications packaging," *IEEE Trans. Microwave Theory Tech.*, vol. 45, pp. 1879–1888, Oct. 1997.

[4] L. Z. Dong, P. S. Hall, and D. Wake, "Dual-frequency planar inverted-F antennas," *IEEE Trans. Antennas Propag.*, vol. 45, pp. 1451–1458, Oct. 1997.

[5] C. R. Rowell and R. D. Murch, "A compact PIFA suitable for dual-frequency 900/1800 MHz operation," *IEEE Trans. Antennas Propag.*, vol. 46, pp. 596–598, Apr. 1998.

[6] M. Ali, "Dual-band antenna having mirror image meandering segments and wireless communicators incorporating same," U.S. Patent 6 184 836, Feb. 6, 2001.

[7] R. Sadler, G. J. Hayes, and M. Ali, "Compact, broadband inverted-f antennas with conductive elements and wireless communicators incorporating same," U.S. Patent 6 218 992, Apr. 17, 2001.

[8] R. Sadler, M. Ali, and G. J. Hayes, "Multi-frequency band inverted-f antennas with coupled branches and wireless communicators incorporating same," U.S. Patent 6 563 466, May 13, 2003.

[9] K. M. Z. Shams and M. Ali, "Study and design of a capacitively coupled polymeric internal antenna," *IEEE Trans. Antennas Propag.*, vol. 53, no. 3, pp. 985–993, Mar. 2005.

[10] M. Z. Azad and M. Ali, "A miniaturized Hilbert PIFA for dual band mobile wireless applications," *IEEE Antennas Wireless Propag. Lett.*, vol. 4, pp. 59–62, 2005.

[11] M. Ali, G. J. Hayes, H. S. Hwang, and R. A. Sadler, "Design of a multi-band internal antenna for third generation mobile phone handsets," *IEEE Trans. Antennas Propag.*, vol. 51, pp. 1452–1461, Jul. 2003.

[12] J. I. Moon and S. O. Park, "Small chip antenna for 2.4/5.8-GHz dual ISM-band applications," *IEEE Antennas Wireless Propag. Lett.*, vol. 2, no. 21, pp. 313–315, 2002.

[13] M. Ali, R. A. Sadler, and G. J. Hayes, "A uniquely packaged internal inverted-F antenna for bluetooth or wireless LAN application," *IEEE Antennas Wireless Propag. Lett.*, vol. 1, no. 1, pp. 5–7, 2002.

[14] M. Ali, T. Sittironnarit, H. S. Hwang, R. A. Sadler, and G. J. Hayes, "Wideband/dual-band packaged antenna for 5–6 GHz WLAN application," *IEEE Trans. Antennas Propag.*, vol. 52, no. 2, pp. 610–615, Feb. 2004.

[15] M. Ali and G. J. Hayes, "A small printed integrated inverted-F antenna for bluetooth application," *Microwave Opt. Technol. Lett.*, vol. 33, no. 5, pp. 347–349, Jun. 5, 2002.

[16] M. Ali, "Miniaturized packaged (embedded) antennas for portable wireless devices," in *Encyclopedia of RF and Microwave Engineering*. New York: Wiley, Feb. 2005, pp. 3068–3082.

[17] C. C. Lin, S. W. Kuo, and H. R. Chuang, "2.4-GHz printed meander-line antenna for WLAN applications," in *IEEE Antennas Propag. Society Int. Symp. Dig.*, June 2004, vol. 3, pp. 2767–2770.

[18] C. M. Su and K. L. Wong, "Narrow flat-plate antenna for 2.4 GHz WLAN operation," *Electron. Lett.*, vol. 39, pp. 344–345, Feb. 2003.

[19] C. M. Su, W. S. Chen, and K. L. Wong, "Compact dual-band metal-plate antenna for 2.4/5.2-GHz WLAN operation," *Microwave Opt. Technol. Lett.*, vol. 38, pp. 113–115, Jul. 2003.

[20] L. S. Tai and H. C. Lin, "Dual-frequency inverted-F antenna," U.S. Patent Appl. 2003/0 234 742 A1, Dec. 25, 2003.

[21] M. Z. Azad and M. Ali, "A miniature Hilbert planar inverted-F antenna (PIFA) for dual-band mobile phone applications," in *IEEE Antennas Propag. Soc. Int. Symp. Dig.*, Jun. 2004, vol. 3, pp. 3127–3130.

[22] C. Puente, J. Romeu, R. Pous, J. Ramis, and A. Hijazo, "Small but long Koch fractal monopole," *Electron. Lett.*, vol. 34, no. 1, pp. 9–10, Jan. 1998.

[23] J. Anguera, C. Puente, E. Martínez, and E. Rozan, "The fractal Hilbert monopole: a two-dimensional wire," *Microwave Opt. Technol. Lett.*, vol. 36, no. 2, pp. 102–104, Jan. 2003.

[24] D. Gala, J. Soler, C. Puente, C. Borja, and J. Anguera, "Miniature microstrip patch antenna loaded with a space-filling line based on the fractal Hilbert curve," *Microwave Opt. Technol. Lett.*, vol. 38, no. 4, pp. 311–312, Aug. 2003.

[25] M. Barra, C. Collado, J. Mateu, and J. M. Callaghan, "Miniaturization of superconducting filters using Hilbert fractal curves," *IEEE Trans. Superconduct.*, vol. 15, pp. 3841–3846, Sep. 2005.

[26] T. Endo, Y. Sunahara, S. Satoh, and T. Katagi, "Resonant frequency and radiation efficiency of meandered line antennas," *Electron. Commun. Jpn.*, vol. 83, no. 1, pt. 2, pp. 52–58, 2000.

[27] B. C. Wadell, *Transmission Line Design Handbook*. Norwood, MA: Artech House, 1991.

[28] F. W. Grover, *Inductance Calculation*. Princeton, NJ: Van Nostrand, 1964.

[29] S. C. K. Ko and R. D. Murch, "Compact integrated diversity antenna for wireless communications," *IEEE Trans. Antennas Propag.*, vol. 49, pp. 954–960, Jun. 2001.

[30] M. Karaboikis, C. Soras, G. Tsachtsiris, and V. Makios, "Compact dual-printed inverted-F antenna diversity systems for portable wireless devices," *IEEE Antennas Wireless Propag. Lett.*, vol. 3, pp. 9–14, 2004.

[31] Y. Ge, K. P. Esselle, and T. S. Bird, "E-shaped patch antennas for high-speed wireless networks," *IEEE Trans. Antennas Propag.*, vol. 52, pp. 3213–3219, Dec. 2004.

[32] M. G. Douglas, M. Okoniewski, and M. A. Stuchly, "A planar diversity antenna for hand-held PCS devices," *IEEE Trans. Veh. Technol.*, vol. 47, pp. 747–754, Aug. 1998.

[33] R. G. Vaughan and J. B. Andersen, "Antenna diversity in mobile communications," *IEEE Trans. Veh. Technol.*, vol. VT-36, pp. 149–172, Nov. 1987.

Mohammed Ziaul Azad (S'05) was born in Dhaka, Bangladesh, in 1977. He received the B.Sc degree in electrical engineering from Bangladesh University of Engineering and Technology, Dhaka, in 2002. He is currently pursuing the Ph.D. degree in electrical engineering at the University of South Carolina, Columbia.

He is the author or coauthor of several refereed journal articles and conference papers. His research interests include antenna miniaturization, diversity antennas, mobile phone and wireless local-area network antennas, GPS antennas, electromagnetic bandgap structures, and their antenna applications.

Mohammod Ali (M'93–SM'03) received the B.Sc. degree in electrical and electronic engineering from the Bangladesh University of Engineering and Technology, Dhaka, in 1987, and the M.A.Sc. and Ph.D. degrees in electrical engineering from the University of Victoria, Victoria, BC, Canada, in 1994 and 1997, respectively.

He was with the Bangladesh Institute of Technology, Chittagong, from 1988 to 1992. From 1998 to 2001, he was with Ericsson Inc., Research Triangle Park, NC, first as a Staff Engineer and then as a Senior Staff Engineer. Since August 2001, he has been with the Department of Electrical Engineering, University of South Carolina, Columbia, where currently he is an Assistant Professor. He was a Visiting Research Scientist with the Motorola Corporate EME Research Laboratory, Plantation, FL, during June to August 2004. He is the author/coauthor of more than 80 refereed journal and conference publications and has received five U.S. patents. His research interests include miniaturized packaged (embedded) antennas, metamaterials and their antenna applications, distributed wireless sensors and rectennas, reconfigurable antennas, and portable/wearable antennas and their interactions with humans (SAR).

Dr. Ali received the 2003 National Science Foundation Faculty Career Award. He received the College of Engineering and Information Technology Young Investigator Award from the University of South Carolina in 2006.